9338 *Macromolecules* **2009**, *42*, 9338–9343
DOI: 10.1021/ma9017372

Macromolecules
ARTICLE

Single Molecule Adhesion Mechanics on Rough Surfaces

Michael Geisler,[†,‡] Dominik Horinek,[‡] and Thorsten Hugel*[,†,‡,⊥]

[†]*IMETUM,* [‡]*Physics Department, CeNS, and* [⊥]*CIPSM, Technische Universität München, 85748 Garching, Germany.* [⊥]*Present address: IMETUM, Boltzmannstrasse 11, 85748 Garching, Germany.*

Received August 4, 2009; Revised Manuscript Received October 29, 2009

ABSTRACT: The nanostructure of materials is supposed to affect polymer adhesion at the solid/liquid interface by variations of the exposed surface area. In contrast, our studies on the nanotribology of single recombinant spider silk proteins onto smooth and rough surfaces made of surgical stainless steel show no effect of the surface morphology. This is explained by the velocity dependence of the desorption process, which reveals a negligible friction and a high in-plane mobility at the molecular scale. We compare our results to all atomistic molecular dynamics simulations that allow estimating an upper limit for the molecular friction coefficient.

Introduction

Nanoscopic modifications of surface morphology are state of the art in many fields, ranging from materials science, through medicine, to nutrition science. They aim at controlling the interaction of macromolecules at the solid/aqueous interface. Colloid stabilization, polymeric lubrication, adhesive bonding, and drug release, to name but a few, make use of nanostructures to design molecular adhesion properties. Up to now studies on the influence of surface structure on polymer, cell, or bacteria adhesion have focused on the number of cells or organisms,[1,2] the mass and conformation of polypeptides,[3] and the interactions of polymer layers with a solid substrate.[4−6] The adsorption and desorption kinetics under force for different surface morphologies have not to our knowledge been systematically addressed at the single molecule level.

For this purpose, we developed an AFM-based single molecule sensor, which is capable of quantifying the molecular adsorption free energy of a single polymer at the solid/liquid interface to gain a better understanding of adhesion phenomena on the molecular scale.[7] We performed different measurements on surgical stainless steel surfaces of varying roughness with one and the same probe molecule. Stainless steel is one of the most prevalent implantable materials, in particular in cardiologic and orthopedic interventions.[8] Microporous steel surfaces, like those investigated here, are a promising approach for controlled drug deposition and retarded drug release.[9]

The effect of the nanoscale roughness on the equilibrium adhesion of a single recombinant spider silk protein eADF-4 (C16)[10] (*Araneus diadematus* fibroin) was determined. Recombinant eADF-4 exhibits no intrinsic structure in aqueous solution.[11] No dependence on nanoscale topography of the substrate is found. We identify the origin of this insensitivity to surface structure to be a high in-plane mobility of the macromolecule at the interface.

Experimental Section

Hydrogenated Polycrystalline Diamond. Hydrogenation of polished polycrystalline diamond surfaces (ElementSix Advancing Diamond Ltd., UK) was conducted as described elsewhere.[12] The samples were heated in a vacuum chamber to a temperature of 700 °C at a pressure of 5×10^{-7} mbar. The hot sample surface was exposed to hydrogen radicals generated by two 2000 °C hot tungsten filaments for 30 min at a constant pressure of 1.5 mbar and cooled in a hydrogen atmosphere. The H-terminated diamond surfaces were hydrophobic with contact angles between 80° and 90°. The specimens were wiped clean followed by ultrasonic cleaning in acetone, 2-propanol, and water before measurements.

Polished and Microporous Surgical Stainless Steel. Circular flat blanks were jet cut from a metal sheet of stainless steel 316 L of 1 mm thickness (Max Cochius GmbH, Munich, Germany) and dressed to a size of 10 mm diameter. To achieve a reduced roughness in the nanometer regime, the samples were grinded with a wet silicon carbide grinding wheel for 2 min at 300 rpm with a constant force of 2 N and polished in several steps at 150 rpm for 2 min with a final polish grain size of 40 nm. In-between the grinding steps the samples were cleaned in an ultrasonic bath for 5 min in deionized water in order to avoid particle transfer from one polish to the other. Specimens with rough surfaces were obtained by a treatment according to the manufacturing process of the PEARL-surface of the YUKON^{DES} stent (Translumina GmbH, Hechingen, Germany).

Scanning Electron Microscopy (SEM). Images of specimens made of surgical stainless steel were acquired by the analysis of the reflected secondary electron beam in a Hitachi S 3500-N scanning electron microscope (SEM). The SEM was operated at an acceleration voltage of 15 keV. Sputter coating of the samples with gold was not necessary due to the good conductivity of the metal surface. Images were taken at representative areas of the polished and microporous steel surfaces to document the roughening effect of the surface treatment.

Atomic Force Microscopy (AFM). For atomic force microscopy (AFM) we used a Molecular Force Probe 3D (MFP-3D, Asylum Research, Santa Barbara, CA) and triangular silicon nitride cantilevers with a nominal spring constant of ∼2 N/m and a resonance frequency of ∼70 kHz (AC240TS, Olympus, Japan). The sample surfaces were imaged by AFM in intermittent contact mode (AC mode) at ambient temperatures in air. The imaging set point was chosen so that the forces acting on the cantilever during imaging were repulsive (beyond the attractive regime). In the case of polished polycrystalline diamond, images were taken in contact mode at a scan rate of 0.6 Hz with

*Corresponding author: e-mail Thorsten.hugel@ph.tum.de; Tel +49 89 289 16781; Fax +49 89 289 10805.

 Published on Web 11/11/2009

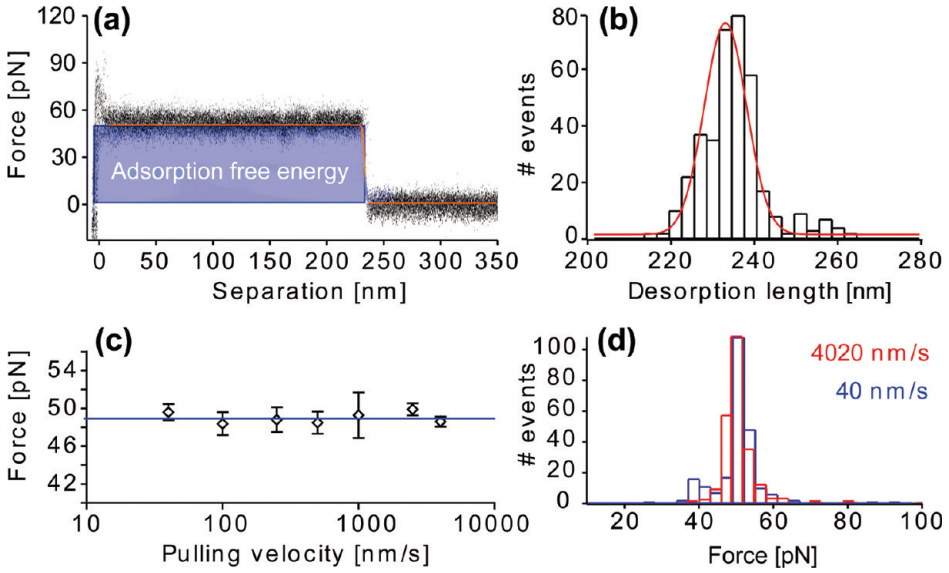

Figure 1. (a) Superposition of 20 typical force−separation traces of eADF-4 on H-terminated diamond. The detachment of the molecule from the surface is indicated by a sudden drop of the force plateau to the zero line (at around 230 nm). The area under the sigmoidal fit to the trace (orange) gives the adsorption free energy per molecule. (b) Gaussian distributed desorption length is sharply peaked and reproduces the molecular length of eADF4 (plus PEG spacer) very well. (c) The mean desorption force derived from distributions of likewise Gaussian shape (d) is independent of pulling speed.

appropriate cantilevers (OMCL-RC800PSA, Olympus, Japan). Image resolution was set to 512 × 512 data points. The roughness of the different materials was calculated from 50 μm × 50 μm sized surface sections, and values for the root-mean-square roughness (R_q) were derived from the AFM height image data.

Single Molecule Force Spectroscopy (SMFS). Preparation of AFM tips (MLCT-AUHW, Veeco GmbH, Germany) and covalent bonding of the N-terminal amine of eADF-4 to the tip using a long, flexible linker of poly(ethylene glycol), PEG (65 kDa, Rapp Polymere, Germany), to avoid interference by direct tip−substrate interactions, is described elsewhere.[7] The molecule is adsorbed at the surface while in contact with the solid for 1 s. By retracting the cantilever, we pulled the protein from the surface at a constant velocity of 1 μm/s. Such approach−retract cycles were performed up to 1000 times at different positions within one measurement. Force−separation traces were derived from the deflection-piezopath signal.[13] The sampling rate was set to 5×10^6 Hz.

The optical lever sensitivity was averaged over the first five and the last five retraction curves. The spring constant of each cantilever was determined before the measurement by integrating over the power spectral density from 75 Hz to the local minimum between the first and the second resonance peak and by applying the equipartition theorem.[14] In doing so, we obtain a spring constant of 20.3 pN/nm (triangular lever).

Comment on Uncertainties of Force Values. Each force value in this study was determined from a histogram built from at least 500 force−separation traces recorded with one and the same molecule (Figure 1d). The corresponding standard deviations were calculated according to the theory of small samples.[15] The main uncertainty stems from cantilever calibration.[16] We therefore used one and the same cantilever to obtain all data points. The uncertainties given in the main text (error bars in Figure 1c) thus do not give the uncertainties of absolute values but rather represent the relative error of the measurements.

Results and Discussion

Macromolecular Friction. Figure 1a shows the superposition of 20 representative force−separation traces obtained by single molecule force spectroscopy (SMFS) of eADF-4 in aqueous NaCl solution on hydrogenated diamond. Adhesion measurement of the single molecule at the interface is not disturbed by cavitation as it is in more macroscopic force detecting devices.[17] The resulting desorption of a single molecule is represented by a plateau of constant force, the length of which approximates the polymer contour length.[18] By taking advantage of this characteristic, the genetically engineered spider silk molecule is clearly identified by its well-defined length (Figure 1b). The desorption length of eADF-4 is Gaussian distributed (Figure 1b) and sharply peaked.

The mean desorption length of 231 nm amounts to 89% of the expected polymer contour length of eADF4 (210 nm) plus PEG spacer (49 nm) in its fully stretched conformation. This is in good agreement with previous experiments on eADF-4[7] and theoretical estimates based on the freely jointed chain model including ab initio quantum mechanical elasticity.[19] The slight deviation from the total contour length is caused by conformational chain fluctuations during desorption. As can be seen from Figure 1c,d, the mean force obtained from Gaussian distributions is not velocity dependent, but rather stays constant over a wide range of pulling speeds. This observation points to a negligible molecular friction and absent energy dissipation of eADF-4 on H-terminated diamond. This finding is corroborated in Figure 2, where a single eADF-4 molecule is partially desorbed from a diamond surface and afterward readsorbed. Starting with the molecule in its adsorbed state, the AFM tip was moved away from the surface, leaving about 120 nm of the polymer chain (about half the polymer contour length) adsorbed at the surface (time index 0 s).

The tip was further retracted 80 nm with 1 μm/s (1) and moved again the same distance toward the surface with the same velocity (2). After that we waited for 7 s (0 μm/s) while the molecule was stretched between surface and tip apex (3). Finally, we performed another retract−approach cycle over a distance of 80 nm at a third velocity of 4 μm/s (4, 5). During this procedure the recorded plateau force remained constant until the force suddenly dropped to the zero line in a single step, indicating a single protein detaching from the surface. Note that the recorded force likewise acts on the cantilever during readsorption (v−) as it does during desorption (v+)

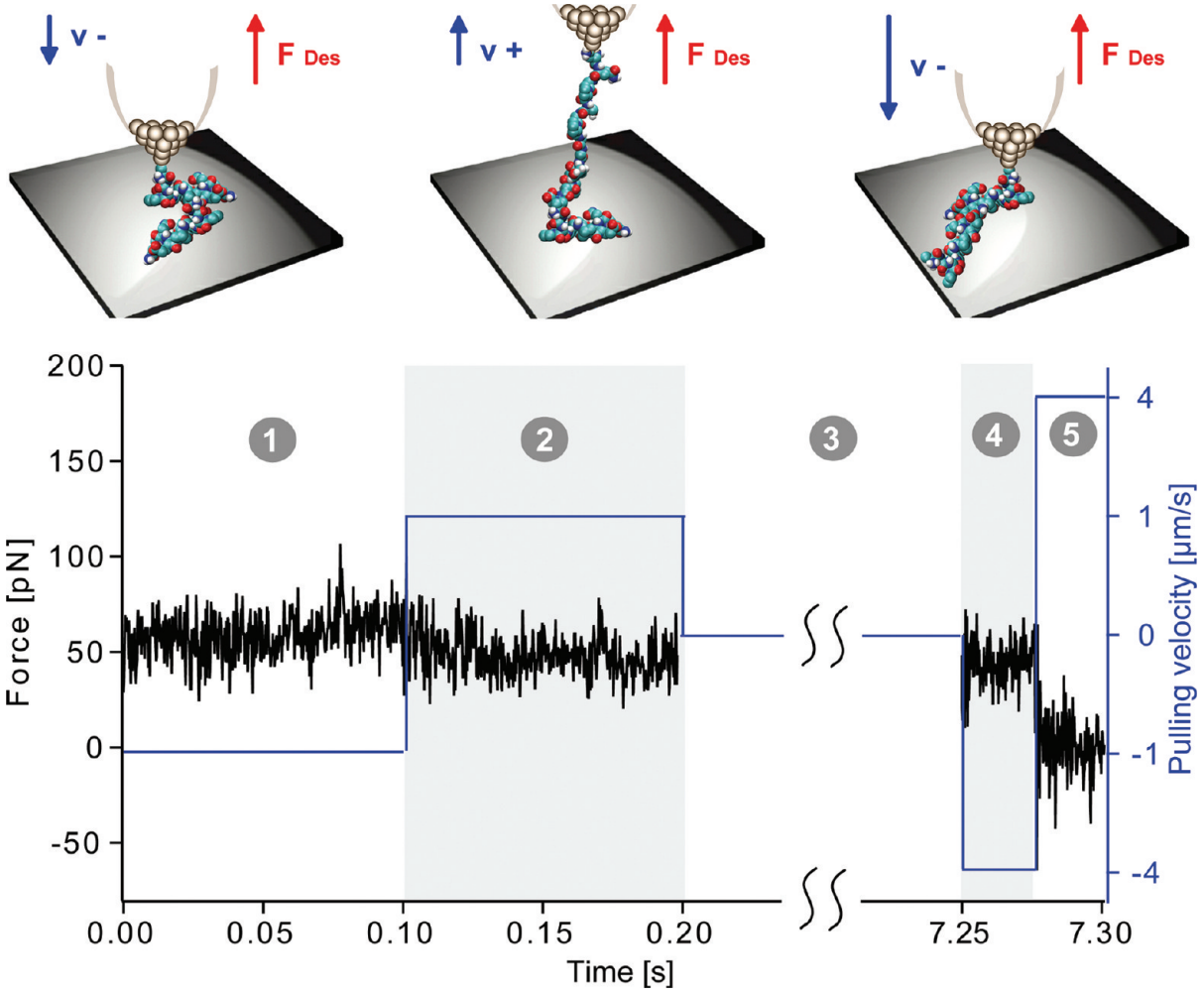

Figure 2. Scheme of a retract-approach cycle with eADF-4 bound to the AFM tip and adsorbed onto the substrate. During desorption, the force plateau is affected neither by pulling speed nor by pulling direction.

and is therefore independent not only from pulling velocity but also from pulling direction. These results imply that the adsorbed chain section reaches equilibrium on the time scales of the experiment and define the observed force plateaus as equilibrium desorption. As long as velocity-independent force plateaus are obtained, molecular friction is low and lateral movement is not constrained. Neglecting the polymeric response in the stretched state, the molecular adsorption free energy corresponds to the area under the force plateau (Figure 1a). Except for a small entropic conformational contribution,[20] the average adsorption free energy per amino acid ω amounts to $\omega = l_a \times$ force with l_a being the amino acid length of 0.365 nm.[21]

To elucidate the influence of the surface structure on polymer−surface interactions comprising adhesion and friction, we performed SMFS on a single eADF4 molecule in aqueous PBS solution (Dulbecco's phosphate buffered saline) at 36.5 °C and determined its adsorption free energy on polished and microporous steel surfaces.

Effect of Surface Roughness. Parts a and f of Figure 3 show electron micrographs of polished and microporous surgical stainless steel 316L, respectively, at 1200× magnification. Polishing of the steel blanks resulted in smooth and homogeneous surfaces with no larger cavities. Some pits that appear as darker spots surrounded by brighter rings are similar in size to the particles of the polish and can be attributed to abrasion. Because in the AFM experiments the approach of the cantilever to the sample surface was monitored by optical microscopy of comparable magnification, those pits were avoided in SMFS experiments. In contrast to polished 316L, the microporous surface exhibits sharp edges and porelike structures uniformly distributed over the whole surface. The topography on smaller scales was obtained with an AFM on the same samples used for SMFS and confirmed the considerable differences in topography for the investigated specimens (Figure 3b,g). The values of the root-mean-square roughness, R_q, were determined from 50 μm × 50 μm sized AFM height images. For polished and microporous steel, R_q was 13 and 494 nm, respectively. Cross-section profiles of the two steel surfaces at the micrometer scale are depicted in Figure 3c,h and at the nanoscale in Figure 3d,i. They illustrate that the difference in roughness continues on the molecular length scale (of the order of the Kuhn length of the polymer) and is therefore comparable or even smaller than the size of the polymer. This is supposed to affect the interaction of biopolymers with the surface due to an increased effective surface area and surface tension.[22]

We observe plateaus of constant force free of hysteresis on steel of either surface roughness (Figure 3e,j) similar to those on hydrogenated diamond in Figure 1a. The measured desorption forces and adsorption free energies of eADF-4 on polished ($7.5 \pm 0.1\ k_BT$; $1\ k_BT$ equals about 2.5 kJ/mol) and microporous stainless steel ($7.6 \pm 0.1\ k_BT$) exhibit no difference for either type of roughness, although the roughness on the nanometer scale relevant

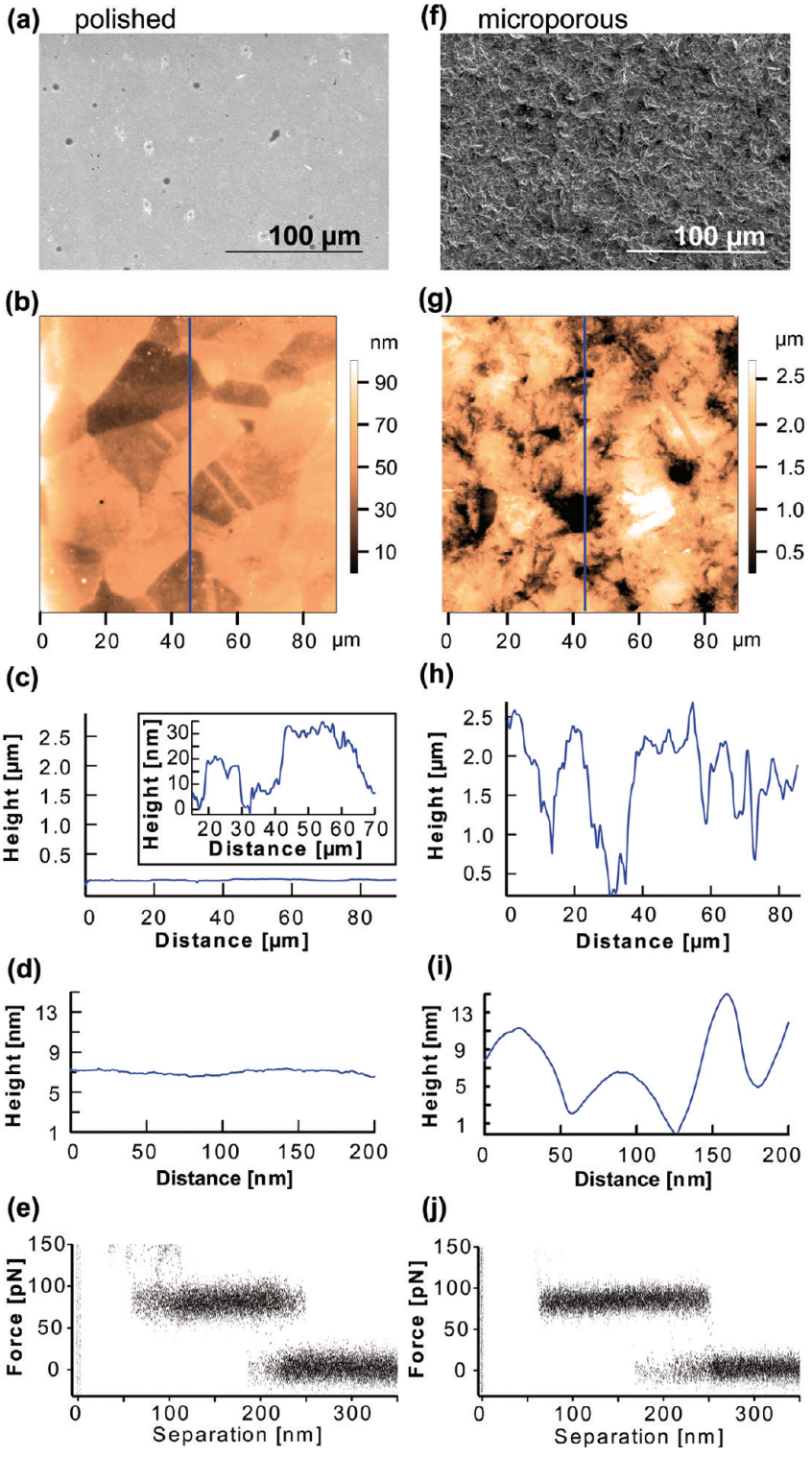

Figure 3. SEM (a) and AFM images (b) of a polished surface of surgical stainless steel blanks. The corresponding profile for a $50 \times 50\,\mu m^2$ area image (b) is depicted in (c) and for a detailed scan of 200×200 nm^2 in (d). The inset in (c) shows a zoom into the height scale. (e) Superposition of 20 force plateaus of eADF-4 on polished steel. The corresponding images for a microporous stainless steel surface are illustrated in (f)−(j).

for molecular interaction differs by a factor of 20. Clearly, our results reveal that there are no pinning points such as directional bonds or increased electrostatic interactions present at the surface. Thus, a possible enhancement of surface adhesion of the mildly negatively charged eADF4 (C_{16}) (in total 16 glutamic acid residues that can carry a charge at pH 7.4) on the rough metal oxide by charged edges can be excluded.

From a macroscopic point of view, an increase in the effective surface area by increasing the surface roughness is supposed to enhance adhesion in different ways. For example, the mechanical anchoring via surface voids and pores is often associated with a stabilization caused by polymer entanglement.[23] Entanglement as well as mechanical and diffusive adhesion describe interactions in a polymer film and do not apply to an isolated molecule. Here we probe the

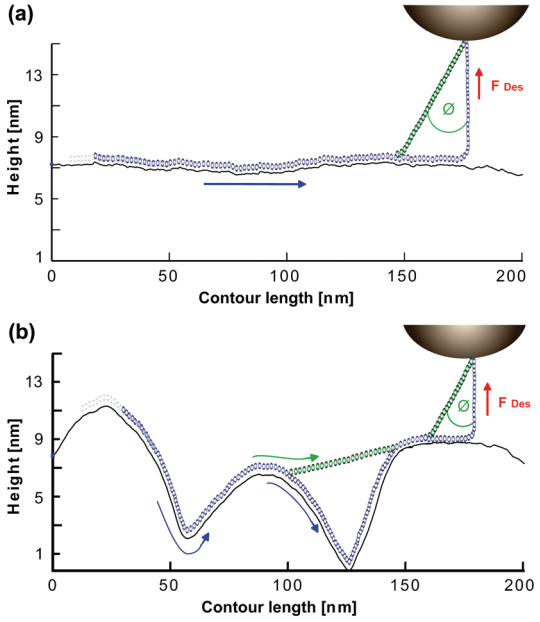

Figure 4. Schematic view of AFM polymer desorption of a polymer along its contour on polished (top) and microporous (bottom) steel. The polymer is drawn to scale, assuming a length of 0.4 nm for an amino acid of a polypeptide. The polymers are desorbed by an AFM tip that moves perpendicularly away from the surface (direction of the red arrows). For both surfaces we show the low friction case (a, $\varphi \approx 0$) and the high friction case (b, $\varphi > 0$). Note that molecular friction depends on the length of the adsorbed polymer chain.

influence of surface structure on the dispersive adhesion of a single polymer. The seemingly counterintuitive results we obtained point to a molecular adhesion mechanism with negligible topographic and friction effects on interactions at the molecular scale.

Molecular Dynamics Simulations. Further evidence for the absence of friction in the SMFS data is drawn from fully atomistic molecular dynamics simulations with explicit water. The lateral motion of spider silk fragments under the influence of an AFM tip was studied on hydrogenated (hydrophobic) and oxidized (hydrophilic) diamond surfaces.[24,25] The hydrophobic surface serves as a model system for surfaces that do not bear any local binding sites, whereas the hydrophilic surface provides local binding sites in the form of hydroxyl groups. These have the ability to form localized hydrogen bonds with the spider silk molecule. From the simulation results[25] it can be inferred that in SMFS experiments of eADF4 composed of 575 amino acids with a total contour length $L = 210$ nm with a pulling rate of 1 μm/s the expected friction forces are 2 fN on the hydrophobic surface and 60 fN on the hydrophilic surface. The presence of hydrogen-bonding sites on the surface thus results in a 30-fold increase in the friction force, but friction effects still remain a negligible contribution to the overall desorption force.

Single Molecule Adhesion and Mobility. In the case of negligible friction, the polymer maximizes its contact area to the surface under the constraint that its end is attached to the AFM tip. Here, we presume that the system is given enough time to equilibrate as evidenced by our experiments. For unfavorable entropies balancing enthalpies favorable for adsorption, the polymer might exhibit a more complex conformation when making contact with the surface. Such partially folded segments forming loops in solution perpendicular to the surface plane are not considered in the following discussion, and we can define an angle ϕ between the desorbed part of the polymer and the surface normal (Figure 4). The polymer will be peeled off vertically in case of vertical cantilever motion. For non-negligible friction, the angle ϕ will deviate from zero. For a constant tip velocity v_z the sliding friction coefficient per unit length ζ can be estimated from the experimental data according to $\gamma = v_z \zeta L/\omega$, where L is the contour length on the surface and ω is the adsorption free energy of the polymer per unit length.[26] Thus, γ is a measure of the ratio of friction vs adsorption strength and thus of the angle ϕ between polymer chain and surface normal. Figure 4 illustrates both scenarios: low friction (blue) and high friction (green). An important result of ref 26 is that, as soon as ϕ deviates detectably from zero, no plateau force will be measured anymore. The authors could show that this is the case for $\gamma < 0.1$. Hence, the upper limit of the friction coefficient becomes $\zeta_{max} \approx 1.3 \times 10^{-8}$ kg/s. The fact that in our observation the force−separation traces always exhibit perfect plateaus signifies that the polymer can freely glide over the surface and that the desorbed polymer chain stays almost vertically ($\phi \approx 0$) aligned between tip and surface (Figure 4a, blue trace).

In the case of a corrugated surface a nonzero attachment angle is of particular interest: as can be seen from Figure 4b, the molecule fills the pores of the rough surface as long as the angle ϕ is very small (blue trace).

However, at a higher friction (which was not observed in the present case) the polymer would desorb from concave regions on the surface during movement and thus leave uncovered voids at the topographic pits (green trace). The latter would have a significant impact on the failure of an adhesive joint at the material interface.

Finally, the binding of the spider silk to metal is expected to occur mainly via hydrogen bonds. These bonds have a typical strength of several $k_B T$ and a typical time scale for bond breaking that is low enough to allow for equilibrium conditions to be achieved in the single-molecule experiment. Pinning points with higher adhesion strength and much slower dynamics would be necessary to observe friction effects at the single-molecule level. As we do not observe friction effects on surfaces of either roughness, we can conclude that a boss or a dip in the surface does not create spots, where increased hydrogen bonding can strongly bind an amino acid of the protein and thus increase the force necessary to desorb the molecule.

In summary, Figure 4 illustrates our picture for the projection along the polymer contour in case of a polished (top) and a microporous substrate (bottom) with a low ($\phi = 0$) and high ($\phi > 0$) friction coefficient. At low friction, the number of contact sites per monomer is about the same on both surfaces. The derived picture is supported by our finding that the plateau force is independent of pulling velocity and pulling direction, which hints at a negligible friction on the molecular scale. The reported influence of surface structure on cell adhesion or on the adherence of an applied coating might therefore be related to cell morphology, to the mechanical interlock of the adhesive material that fills the voids or pores of the surface, to the stabilization by polymer entanglement, or to the occurrence of specific bonds[25] but, as we have shown here, not to individual polymer−substrate interactions.

Concluding Remarks

Our AFM-based single molecule approach similar to a "nano-peel test" demonstrates negligible friction effects on the adhesion of single polymers on surgical stainless steel independent of the nanoscale roughness. This "sliding adhesion" manifests itself in

similar adsorption free energies per molecule regardless of the surface roughness. The experiments clearly show an equilibrium situation, despite the formation of hydrogen bonds between polymer and surface.

Our results give new insights into effects of topography on the adhesion of single polymers at the solid/liquid interface and will guide the development of functionalized nanomaterials in contact with polymer solutions. In addition, single molecule force sensors like those presented here might evolve to become a powerful tool in materials and surface science, capable of meeting the growing requirements for analyzing instrumentation in nanotechnology.

Acknowledgment. Fruitful discussions with Jürgen Kreuzer, Roland Netz, and Robert Stark are gratefully acknowledged. We thank the Deutsche Forschungsgemeinschaft (DFG), Nanosystems Initiative Munich (NIM), and the Fond der Chemischen Industrie for financial support. M.G. is supported by the Elitenetzwerk Bayern in the framework of the doctorate program Materials Science of Complex Interfaces and the Stiftung Industrieforschung.

References and Notes

(1) Liu, X.; Lim, J. Y.; Donahue, H. J.; Dhurjati, R.; Mastro, A. M.; Vogler, E. A. *Biomaterials* **2007**, *28*, 4535–4550.
(2) Curtis, A.; Wilkinson, C. *Biomaterials* **1997**, *18* (24), 1573–1583.
(3) Han, M.; Sethuraman, A.; Kane, R. S.; Belfort, G. *Langmuir* **2003**, *19* (23), 9868–9872.
(4) Hayashi, T.; Sano, K.; Shiba, K.; Kumashiro, Y.; Iwahori, K.; Yamashita, I.; Hara, M. *Nano Lett*. **2006**, *6* (3), 515–519.
(5) Conti, M.; Donati, G.; Cianciolo, G.; Stefoni, S.; Samori, B. *J. Biomed. Mater. Res*. **2002**, *61* (3), 370–379.
(6) Kidoaki, S.; Matsuda, T. *Langmuir* **1999**, *15* (22), 7639–7646.
(7) Geisler, M.; Pirzer, T.; Ackerschott, C.; Lud, S.; Garrido, J.; Scheibel, T.; Hugel, T. *Langmuir* **2008**, *24* (4), 1350–1355.
(8) Williams, D. F. *Biomaterials* **2008**, *29*, 2941–2953.
(9) Wessely, R.; Hausleiter, J.; Michaelis, C.; Jaschke, B.; Vogesser, M.; Milz, S.; Behnisch, B.; Schratzenstaller, T.; Renke-Gluszko, M.; Stöver, M.; Wintermantel, E.; Kastrati, A.; Schömig, A. *Arterioscle., Thromb., Vasc. Biol*. **2005**, *25*, 748–753.
(10) Vendrely, C.; Scheibel, T. *Macromol. Biosci*. **2007**, *7* (4), 401–409.
(11) Exler, J. H.; Hummerich, D.; Scheibel, T. *Angew. Chem., Int. Ed*. **2007**, *46* (19), 3559–3562.
(12) Hartl, A.; Garrido, J. A.; Nowy, S.; Zimmermann, R.; Werner, C.; Horinek, D.; Netz, R.; Stutzmann, M. *J. Am. Chem. Soc*. **2007**, *129* (5), 1287–1292.
(13) Hugel, T.; Seitz, M. *Macromol. Rapid Commun*. **2001**, *22* (13), 989–1016.
(14) Butt, H. J.; Jaschke, M. *Nanotechnology* **1995**, *6* (1), 1–7.
(15) Spiegel, M. R. *Theory and Problems of Statistics*, 2nd ed.; McGraw-Hill Publishing: New York, 1992; p 512.
(16) Pirzer, T.; Geisler, M.; Scheibel, T.; Hugel, T. *Phys. Biol*. **2009**, *6*, 2.
(17) Meyer, E. E.; Rosenberg, K. J.; Israelachvili, J. *Proc. Natl. Acad. Sci. U.S.A*. **2006**, *103* (43), 15739−15746.
(18) Sonnenberg, L.; Billon, L.; Gaub, H. E. *Macromolecules* **2008**, *41* (10), 3688–3691.
(19) Neuert, G.; Hugel, T.; Netz, R. R.; Gaub, H. E. *Macromolecules* **2006**, 39.
(20) Friedsam, C.; Gaub, H. E.; Netz, R. R. *Europhys. Lett*. **2005**, *72* (5), 844–850.
(21) Hanke, F.; Livadaru, L.; Kreuzer, H. J. *Europhys. Lett*. **2005**, *69* (2), 242–248.
(22) Ji, H.; Hone, D. *Macromolecules* **1988**, *21* (8), 2600–2605.
(23) Cognard, P. *Adhesives and Sealants - General Knowledge, Application Techniques, New Curing Techniques*; Elsevier: Amsterdam, 2006; Vol. *2*, p 512.
(24) Horinek, D.; Serr, A.; Bonthius, D.; Bostrom, M.; Kunz, W.; Netz, R. R. *Langmuir* **2008**, *24* (4), 1271–1283.
(25) Serr, A.; Horinek, D.; Netz, R. R. *J. Am. Chem. Soc*. **2008**, *130* (37), 12408–12413.
(26) Serr, A.; Netz, R. R. *Europhys. Lett*. **2006**, *73* (2), 292–298.